Published in final edited form as:
J Fluoresc. 2013 May ; 23(3): 375–379. doi:10.1007/s10895-013-1161-6.

Long Wavelength Fluorescence Ratiometric Zinc Biosensor

Hui Hui Zeng[1], **Evgenia Matveeva**[1], **Andrea K. Stoddard**[2], **Carol A. Fierke**[2], and **Richard B. Thompson**[1,*]

[1]Department of Biochemistry and Molecular Biology, University of Maryland School of Medicine, 108 N. Greene Street, Baltimore, MD 21201

[2]Department of Chemistry, University of Michigan, 930 W. University Ave., Ann Arbor, MI 47805

Abstract

A protein-based emission ratiometric fluorescence biosensor is described that exhibits sensitivity to free zinc ion solutions down to picomolar concentrations. Ratiometric measurements are widely used to assure accurate quantitation, and emission ratios are preferred for laser scanning microscopes such as confocal fluorescence microscopes. The relatively long emission wavelengths used are well suited to studies in tissues and other matrices which exhibit significant fluorescence background, and the apo-carbonic anhydrase moiety recognizes zinc ion with high and controllable specificity.

Keywords

Zinc ion; fluorescence biosensor; ratiometric; carbonic anhydrase; FRET; Forster resonance energy transfer

Introduction

Over the last few years, several groups have described sensors and indicators for zinc ions in aqueous solution that transduce the presence or level of the ion as a change in a fluorescence observable such as intensity, spectrum, polarization (anisotropy), or lifetime (1–7); reviewed in (8–12). Particularly due to the growing interest in zinc ions in biology and medicine, the development of these sensors and indicators has been spurred by the straightforward ability to map free zinc ion levels by fluorescence microscopy. In these sensors, we and others have emphasized both sensitivity and high selectivity for use in living systems and natural waters (11, 13). Selective organic chelating structures serving as recognition moieties within such fluorescence sensors, including N-(6-methoxy-8-quinolyl)-p-toluenesulfonamide (TSQ) (1), cyclen macrolides (14), and di-2-picolylamine (15, 16) have been described (5) that have high affinity and selectivity for zinc ion in comparison to likely interferents such as Ca(II) or Mg(II). However, these and other chelating moieties are hard to modify to alter affinity, selectivity, and/ or metal binding kinetics for any particular application without changing other properties of the molecule. Instead, we and others have used biological molecules to serve as both recognition moieties and in some cases, fluorescent reporters (17) (18),(19, 20) (21),(22, 23). We have shown that by subtle changes in protein structure the affinity (24, 25), selectivity (26), and even zinc ion binding kinetics (27) can all be optimized for a given application (reviewed in (23, 28). Moreover, the protein- and nucleic acid-based (29) sensors can be expressed within particular tissues, cells, or even organelles of an organism to study zinc ion *in vivo*. We described an excitation-ratiometric fluorescent zinc biosensor based on

*To whom correspondence should be addressed: rthompso@umaryland.edu.

carbonic anhydrase that has proven useful in studying free zinc ion in living cells at picomolar levels (30–32). Excitation ratiometric indicators, like Fura-2 for calcium (33), have proven widely popular for accurate quantitation of metal ions in microscopy, in part because they can be easily used with commonly available xenon lamp excitation, and because there is no issue of image shift due to chromatic aberration since the emission is only observed at a single wavelength. However, microscopes with laser excitation, such as laser scanning confocal microscopes, often cannot rapidly switch between excitation wavelengths, or the needed wavelengths may not be available at all.

A second issue that is of continuing concern in fluorescence studies, particularly of living cells, tissues, and whole organisms, is the presence of background fluorescence, and high optical absorbance and scattering (reviewed in(34) (35, 36) (37). This is of particular concern in performing fluorometry *in vivo*, and a common approach that largely addresses all three issues is to use fluorescent labels and sensors which absorb and emit at longer wavelengths, extending into the infrared; as a result, scores of long wavelength fluorescent labels have been described in the literature, many based on cyanine and squaraine backbones (38–40). Because our earlier excitation ratiometric sensor required ultraviolet excitation, it was subject to these problems and thus less suited for deep tissues or live animals. Thus here we describe a modified emission ratiometric approach usable with longer wavelength (590 nm) excitation.

The sensor function relies on Förster resonance energy transfer (FRET) and is depicted schematically in Figure 1. Briefly, the Alexa Fluor 594 (AF594) covalently attached to carbonic anhydrase acts as fluorescence donor. In the absence of bound zinc ion, AF594 emits at approximately 617 nm. When zinc is present it binds to the apo-CA, and promotes the binding of Chesapeake Blue sulfonamide in the protein active site. CA-bound Chesapeake Blue sulfonamide is located close enough to the AF594 to serve as an energy transfer acceptor; the energy is resonantly transferred by the Förster dipole-dipole mechanism, and emission at 650 nm from the Chesapeake Blue sulfonamide acceptor is observed. The ratio of emission at 617 to that at 650 nm is inversely proportional to the fraction of the protein with zinc bound, and thus reflects the concentration of free zinc ions.

Apo-H36C-AF594 and apo-H36C-AF660

Human carbonic anhydrase II with cysteine replacing histidine at position 36 and serine replacing cysteine at position 206 was cloned and expressed in *E. coli* BL21(DE3) transformed with pACA, isolated and purified, and labeled with Alexa Fluor 594 C_5-maleimide (Invitrogen/Molecular probes catalog number A10256) all essentially as previously described (41).

Synthesis of Chesapeake Blue sulfonamide

Chesapeake Blue sulfonamide was synthesized by condensation of Square-635H-mono-NHS (Seta BioMedicals, Urbana, IL, cat. no. K8-1612) with a 1.2-fold molar excess of 4-(2-aminoethyl)benzenesulfonamide ([CAS no.35303-76-5]; Aldrich cat no. 27524-7) in DMF with 1 mM N,N-(diisopropyl)ethylamine (Sigma-Aldrich cat. No. 550043) to maintain elevated pH with stirring at room temperature for two hours, following the reaction by thin layer chromatography on reverse phase plates eluted with CH_3CN: H_2O 1:4. The reaction was quenched with excess ethanolamine, water was added and the mixture frozen and lyophilized; apparent purity was 75%.

Fluorescence Measurements of Zinc Concentration

Fluorescence spectra were obtained on a Spectronics AB-2 spectrophotofluorometer; concentrations of free zinc were maintained using a zinc buffer system (10 mM MOPS pH

7.0, 2 mM nitrilotriacetic acid (NTA)with $ZnCl_2$ added to provide free [Zn] ranging from 10^{-15} to 10^{-8} M) as previously described (42).

Results and Discussion

Absorbance and fluorescence emission spectra of the Alexa-Fluor 594-labeled carbonic anhydrase and Chesapeake Blue sulfonamide are depicted in Figure 2. The excellent overlap between the Alexa Fluor 594 donor and Chesapeake Blue acceptor is apparent from the spectra and resulted in a calculated Förster distance of XX Å; the relatively small size of the CA molecule means that the distance between the label selectively attached at the engineered cysteine residue at position 36 and the bound Chesapeake Blue acceptor is roughly 24 Å which allows efficient energy transfer, as observed.

Zinc-dependent emission spectra of apo-H36C-AF594 CA in the presence of CB sulfonamide are depicted in Figure 3 the increase in CB sulfonamide emission (670 nm) together with the concomitant decline in AF594 emission (610 nm) indicate the presence of energy transfer, which is confirmed by changes in the acceptor excitation spectra (data not shown). The ratio of emission intensity from the Alexa Fluor 594 label at 610 nm to that of Chesapeake Blue at 680 nm as a function of free zinc concentration is depicted in Figure 4. The ratio declines with increasing free zinc concentration, as expected; notably, the ratio declines by 50% as the binding site becomes saturated. This large ratio change is desirable for accurate measurements, and minimizes the effects of small variations in background fluorescence. A single site binding isotherm fit to these data yields an apparent K_D of 5.8 ± 3.1 pM, in excellent agreement with the published value of 4 pM. We note that the exact value of the ratio depends on both the particular excitation and emission wavelengths used, and the wavelength dependence of the fluorometer or microscope optics and detector. Crosstalk from the Alexa Fluor 594 acceptor may be minimized by monitoring the emission of Alexa Fluor 594 at 610 nm and the Chesapeake Blue emission at 680 nm. Excitation at 590 nm near the peak of Alexa Fluor 594 absorption also directly excites the Chesapeake Blue sulfonamide acceptor with better than 25% of its peak absorbance; excitation of Alexa Fluor 594 at 532 nm reduces the Alexa Fluor absorbance to about 30% of its peak value, but that of the Chesapeake Blue to only 3% of its peak value, reducing the directly excited acceptor contribution to the 680 nm (FRET) emission. In other FRET-based zinc sensors we have found that the apparent K_D for zinc is relatively insensitive to sulfonamide concentration, as long as the total sulfonamide concentration remains near or above the sulfonamide K_D, which is approximately one micromolar. The CB sulfonamide has one positive and three negative charges at neutral pH; therefore we do not anticipate that it will readily enter cells, and unless the fluorescent labeled carbonic anhydrase uses a cellular importation peptide like TAT (43) to facilitate transport, it also is unlikely to enter cells, so as described these sensors are useful for extracellular measurements.

The tunable selectivity, sensitivity, and metal ion binding kinetics of the carbonic anhydrase family represents key advantages for their use in complex matrices such as biological specimens and natural waters (reviewed in (23, 28, 42)). For instance, the wild type zinc ion binding site exhibits picomolar affinity in the example shown in Figure 3, but a protein variant can be substituted having different affinity (44) or selectivity (B. McCranor, et al., submitted), or metal binding kinetics (42) depending upon the particular circumstances and application. Our distinguished colleagues have demonstrated an infrared ratiometric fluorescent zinc sensor (45) with high affinity and selectivity, but changing its affinity, selectivity, or kinetics requires resynthesizing the molecule. Furthermore, the protein-based sensors may be readily expressed within the cell, expressed within a particular subset of cells, or targeted for expression in particular organelles (22, 46); innovative approaches for

doing this have appeared that employ biomolecules conjugated with small molecule indicators (47).

This sensor will be most useful in studying zinc levels and fluxes in tissues and other matrices that have relatively high fluorescence backgrounds. Of course, the basic principle of the sensor can be extended to even longer wavelengths provided that the donor label on the protein transfers well to the sulfonamide acceptor (exhibits a large R_0), which is mainly controlled by the overlap of the donor emission band with the acceptor, the donor quantum yield, and their proximity. The availability of reactive fluorescent labels with emission at wavelengths in the near infrared from Molecular Probes, Li-cor, Dyomics, SETA BioMedicals and other firms will shortly make this a reality (36). Such sensors offer the prospect of *in vivo* imaging of zinc levels and fluxes in living animals under a host of conditions.

Acknowledgments

The authors wish to thank the National Institutes of Health (NIH RO1 EB003924) for their support.

References

1. Frederickson CJ, Kasarskis EJ, Ringo D, Frederickson RE. A quinoline fluorescence method for visualizing and assaying histochemically reactive zinc (bouton zinc) in the brain. Journal of Neuroscience Methods. 1987; 20:91–103. [PubMed: 3600033]
2. Zalewski PD, Forbes IJ, Betts WH. Correlation of apoptosis with change in intracellular labile Zn(II) using Zinquin [(2-methyl-8-p-toluenesulphonamido-6-quinolyloxy)acetic acid], a new specific fluorescent probe for Zn(II). Biochemical Journal. 1993; 296:403–408. [PubMed: 8257431]
3. Thompson RB, Patchan MW. Lifetime-based fluorescence energy transfer biosensing of zinc. Anal Biochem. 1995; 227:123–128. [PubMed: 7668370]
4. Thompson RB, Maliwal BP, Fierke CA. Expanded dynamic range of free zinc ion determination by fluorescence anisotropy. Anal Chem. 1998; 70(9):1749–1754.
5. Hirano T, Kikuchi K, Urano Y, Higuchi T, Nagano T. Highly zinc-selective fluorescent sensor molecules suitable for biological applications. Journal of the American Chemical Society. 2000; 122:12399–12400.
6. Burdette SC, Walkup GK, Spingler B, Tsien RY, Lippard SJ. Fluorescent sensors for Zn(2+) based on a fluorescein platform: synthesis, properties and intracellular distribution. (Translated from eng). Journal of the American Chemical Society. 2001; 123(32):7831–7841. (in eng). [PubMed: 11493056]
7. Gee KR, Zhou ZL, Ton-That D, Sensi SL, Weiss JH. Measuring zinc in living cells. A new generation of sensitive and selective fluorescent probes. Cell Calcium. 2002; 31(5):245–251. [PubMed: 12098227]
8. White, CE.; Argauer, RJ. Fluorescence Analysis: A Practical Approach. Marcel Dekker, Inc; New York: 1970. p. 380
9. Fernandez-Gutierrez, A.; Munoz de la Pena, A. Determinations of inorganic substances by luminescence methods. In: Schulman, SG., editor. Molecular Luminescence Spectroscopy, Part I: Methods and Applications, Chemical Analysis: A Series of Monographs on Analytical Chemistry and its Applications. Vol. 77. Wiley-Interscience; New York: 1985. p. 371-546.
10. Burdette SC, Lippard SJ. ICCC34-golden edition of coordination chemistry reviews. Coordination chemistry fro the neurosciences. Coordination Chemistry Reviews. 2001; 216–217:333–361.
11. Jiang P, Guo Z. Fluorescent detection of zinc in biological systems: recent development on the design of chemosensors and biosensors. Coordination Chemistry Reviews. 2004; 248:205–229.
12. Thompson, RB., et al. Measurement and imaging of free and total zinc in biological specimens. In: Rink, L., editor. Zinc in Human Health. IOS Press; Amsterdam: 2011. p. 163-191.

13. Thompson, RB.; Zeng, HH.; Loetz, M.; Fierke, C. Issues in enzyme-based metal ion biosensing in complex media. In: Cohn, GE., editor. In-vitro Diagnostic Instrumentation. SPIE; 2000. p. 120-127.

14. Koike T, Watanabe T, Aoki S, Kimura E, Shiro M. A Novel Biomimetic Zinc(II) Fluorophore, Dansylamidoethyl Pendant Macrocyclic Tetraamine 1,4,7,10-Tetraazacyclododecane (Cyclen). Journal of the American Chemical Society. 1996; 118(50):12696–12703.

15. Haugland, RP., editor. Handbook of Fluorescent Probes and Research Chemicals. 6. Molecular Probes, Inc; Eugene, Oregon: 1996. p. 679

16. Walkup GK, Burdette SC, Lippard SJ, Tsien RY. A new cell-permeable fluorescent probe for Zn2+ Journal of the American Chemical Society. 2000; 122:5644–5645.

17. Thompson RB, Jones ER. Enzyme-based fiber optic zinc biosensor. Anal Chem. 1993; 65:730–734.

18. Walkup GK, Imperiali B. Fluorescent chemosensors for divalent zinc based on zinc finger domains. Enhanced oxidative stability, metal binding affinity, and structural and functional characterization. Journal of the American Chemical Society. 1997; 119:3443–3450.

19. Jensen KK, Martini L, Schwartz TW. Enhanced fluorescence resonance energy transfer between spectral variants of green fluorescent protein through zinc-site engineering. Biochemistry. 2001; 40:938–945. [PubMed: 11170415]

20. Qiao W, Mooney M, Bird AJ, Winge DR, Eide DJ. Zinc binding to a regulatory zinc-sensing domain monitored in vivo by using FRET. Proceedings of the National Academy of Sciences. 2006; 103(23):8674–8679.

21. Dongen, EMWMv, et al. Variation of linker length in ratiometric fluorescent sensor proteins allows rational tuning of Zn(II) affinity in the picomolar to femtomolar range. Journal of the American Chemical Society. 2007; 129:3494–3495. [PubMed: 17335212]

22. Qin Y, Dittmer PJ, Park JG, Jansen KB, Palmer AE. Measuring steady-state and dynamic endoplasmic reticulum and Golgi Zn2+ with genetically encoded sensors. Proceedings of the National Academy of Sciences. 2011

23. Hurst TK, Wang D, Thompson RB, Fierke CA. Carbonic anhydrase II-based metal ion sensing: Advances and new perspectives. Biochimica et Biophysica Acta (BBA) - Proteins & Proteomics. 2010; 1804(2):393–403.

24. Kiefer LL, Ippolito JA, Fierke CA, Christianson DW. Redesigning the zinc binding siteof human carbonic anhydrase II: Structure of a His2Asp-Zn2+ metal coordination polyhedron. Journal of the American Chemical Society. 1993; 115:12581–12582.

25. Kiefer LL, Paterno SA, Fierke CA. Hydrogen bond network in the metal binding site of carbonic anhydrase enhances zinc affinity and catalytic efficiency. Journal of the American Chemical Society. 1995; 117:6831–6837.

26. Hunt JA, Ahmed M, Fierke CA. Metal binding specificity in carbonic anhydrase is influenced by conserved hydrophobic amino acids. Biochemistry. 1999; 38:9054–9060. [PubMed: 10413479]

27. Huang, C-c; Lesburg, CA.; Kiefer, LL.; Fierke, CA.; Christianson, DW. Reversal of the hydrogen bond to zinc ligand histidine-119 dramatically diminishes catalysis and enhances metal equilibration kinetics in carbonic anhydrase II. Biochemistry. 1996; 35(11):3439–3446. [PubMed: 8639494]

28. Fierke CA, Thompson RB. Fluorescence-based biosensing of zinc using carbonic anhydrase. Biometals. 2001; 14(3–4):205–222. [PubMed: 11831457]

29. Yang, L.; Ellington, AD. Prospects for the de novo design of nucleic acid biosensors. In: Thompson, RB., editor. Fluorescence Sensors and Biosensors. CRC Press; Boca Raton, FL: 2005.

30. Bozym RA, Thompson RB, Stoddard AK, Fierke CA. Measuring Picomolar Intracellular Exchangeable Zinc in PC-12 Cells Using a Ratiometric Fluorescence Biosensor. ACS Chem Biol. 2006; 1(2):103–111. [PubMed: 17163650]

31. Wang D, Hurst TK, Thompson RB, Fierke CA. Genetically encoded ratiometric biosensors to measure extracellular exchangeable zinc in Escherichia coli. Journal of Biomedical Optics. 2011; 16(8):087011-087011–087011-087011. [PubMed: 21895338]

32. McCranor BJ, et al. Quantitative imaging of mitochondrial and cytosolic free zinc levels in an in vitro model of ischemia/reperfusion. (Translated from eng). J Bioenerg Biomembr. 2012; 44(2): 253–263. (in eng). [PubMed: 22430627]
33. Grynkiewicz G, Poenie M, Tsien RY. A new generation of calcium indicators with greatly improved fluorescence properties. Journal of Biological Chemistry. 1985; 260(6):3440–3450. [PubMed: 3838314]
34. Wolfbeis, OS. The fluorescence of organic natural products. In: Schulman, SG., editor. Molecular Luminescence Spectroscopy Methods and Applications: Part I, CHemical Analysis: A series of monographs on analytical chemistry and its applications. Wiley-Interscience; New York: 1985. p. 167-370.
35. Heong CWF, Prahl SA, Welch AJ. A review of the optical properties of biological tissues. IEEE Journal of Quantum Electronics. 1990; QE-26:2166–2185.
36. Thompson, RB. Red and near-infrared fluorometry. In: Lakowicz, JR., editor. Topics in Fluorescence Spectroscopy Vol. 4: Probe Design and Chemical Sensing. Vol. 4. Plenum Press; New York: 1994. p. 151-181.
37. Ntziachristos V. Fluorescence molecular imaging. Annual Review of Biomedical Engineering. 2006; 8:1–33.
38. Mujumdar RB, Ernst LA, Mujumdar SR, Lewis CJ, Waggoner AS. Cyanine dye labeling reagents: sulfoindocyanine succinimidyl esters. Bioconjug Chem. 1993; 4(2):105–111. [PubMed: 7873641]
39. Narayanan N, Patonay G. A New Method for the Synthesis of Heptamethine Cyanine Dyes: Synthesis of New Near-Infrared Fluorescent Labels. The Journal of Organic Chemistry. 1995; 60(8):2391–2395.
40. Terpetschnig E, Szmacinski H, Ozinskas A, Lakowicz JR. Synthesis of squaraine-N-hydroxysuccinimide esters and their biological application as long-wavelength fluorescent labels. Anal Biochem. 1994; 217(2):197–204. [PubMed: 8203747]
41. Zeng HH, et al. Real-time determination of picomolar free Cu(II) in seawater using a fluorescence-based fiber optic biosensor. Anal Chem. 2003; 75(24):6807–6812. [PubMed: 14670039]
42. Bozym, R., et al. Determination of zinc using carbonic anhydrase-based fluorescence biosensors. In: Brand, L.; Johnson, M., editors. Fluorescence Spectroscopy, Methods in Enzymology. Vol. 450. Academic Press; San Diego: 2008. p. 287-309.
43. Schwarze SR, Ho A, Vocero-Akbani A, Dowdy SF. In vivo protein transduction: Delivery of a biologically active protein into the mouse. Science. 1999; 285:1569–1572. [PubMed: 10477521]
44. Zeng, H-H., et al. In situ measurement of free zinc in an ischemia model and cell culture using a ratiometric fluorescence-based biosensor. In: Vo-Dinh, T.; Grundfest, WS.; Benaron, DA.; Cohn, GE., editors. SPIE Conference on Advanced Biomedical and CLinical Diagnostic Systems III. SPIE; 2005. p. 51-59.
45. Kiyose K, Kojima H, Urano Y, Nagano T. Development of a ratiometric fluorescent zinc ion probe in near-infrared region, based on tricarbocyanine chromophore. Journal of the American Chemical Society. 2006; 128:6548–6549. [PubMed: 16704241]
46. McCranor B, et al. Quantitative imaging of mitochondrial and cytosolic free zinc levels in an in vitro model of ischemia/reperfusion. J Bioenerg Biomembr. 2012; 44(2):253. [PubMed: 22430627]
47. Tomat E, Nolan EM, Jaworski J, Lippard SJ. Organelle-Specific Zinc Detection Using Zinpyr-Labeled Fusion Proteins in Live Cells. Journal of the American Chemical Society. 2008; 130(47): 15776. [PubMed: 18973293]

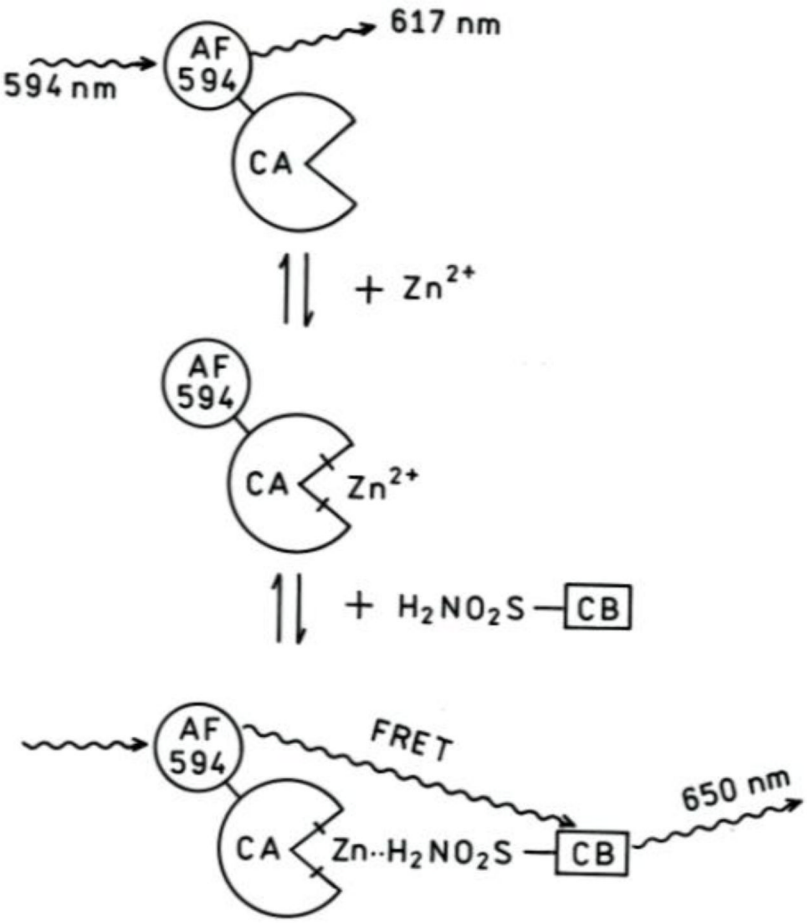

Figure 1.
Principle of the sensor

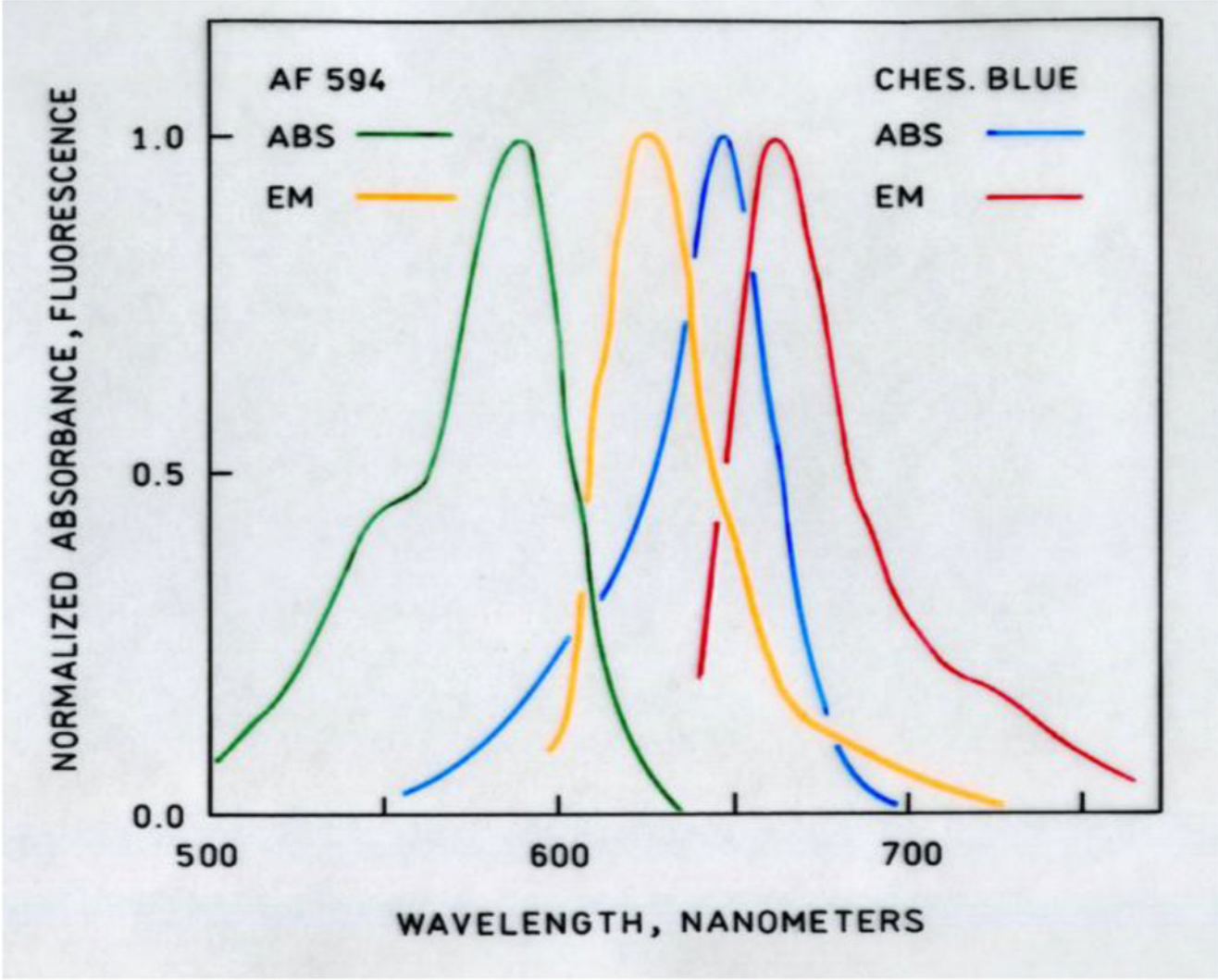

Figure 2.
Normalized absorbance and emission spectra of Alexa Fluor 594(—, —) and Chesapeake Blue sulfonamide (—, —).

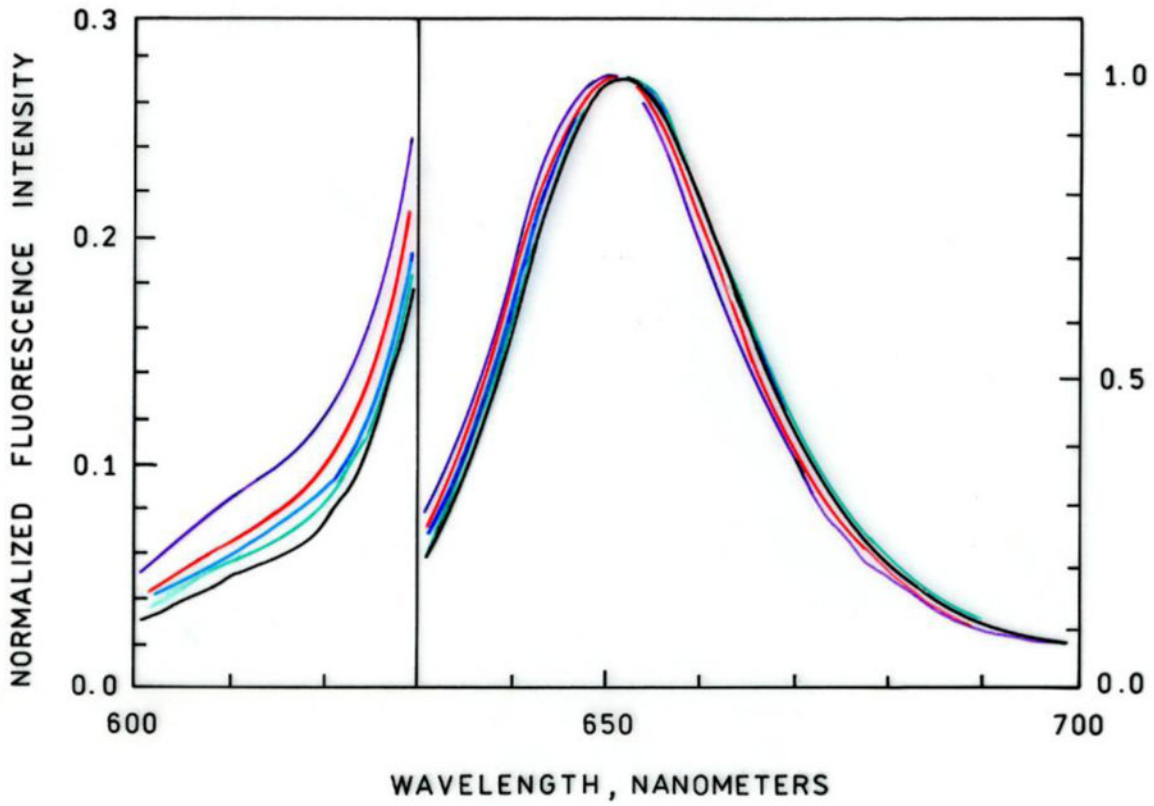

Figure 3.

Zinc-dependent normalized fluorescence emission spectra of apo-H36C-AF594 CA plus Chesapeake Blue sulfonamide. From top to bottom at 610 nm, $[Zn^{2+}]_{FREE}$ = 0.2, 1.06, 10.7, 55, 2000 pM. Note change in Y-axis scale at 630 nm; excitation at 590 nm.

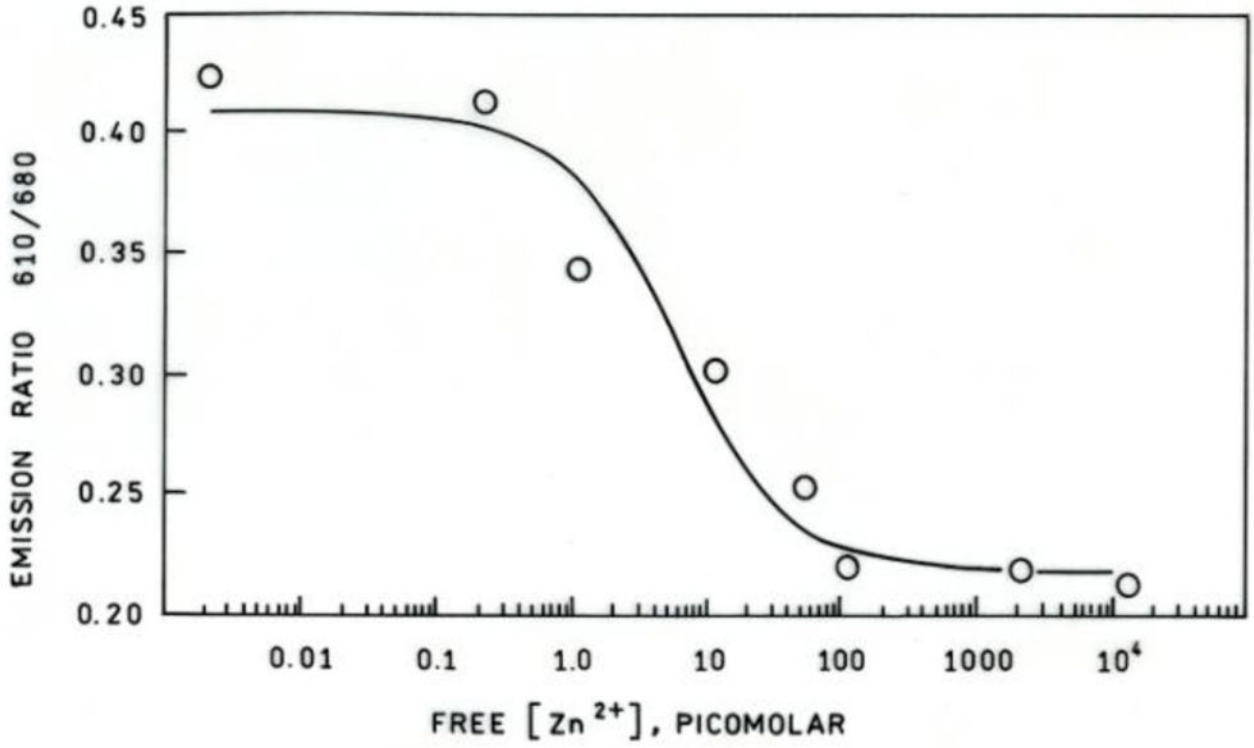

Figure 4.
Fluorescence emission ratio (○) as a function of free zinc concentration maintained using a MOPS/NTA buffer at pH 7.5 for 2 uM H36C-AF594 CA plus 5 uM Chesapeake Blue sulfonamide, together with the best fit binding isotherm.